INFECTION AND IMMUNITY, July 2007, p. 3220–3232 Vol. 75, No. 7
0019-9567/07/$08.00+0 doi:10.1128/IAI.00072-07

Identification of Transferrin-Binding Domains in TbpB Expressed by *Neisseria gonorrhoeae*▽

Amanda J. DeRocco and Cynthia Nau Cornelissen*

Department of Microbiology and Immunology, Virginia Commonwealth University Medical Center, Richmond, Virginia 23298-0678

Received 12 January 2007/Returned for modification 7 March 2007/Accepted 9 April 2007

The transferrin iron acquisition system of *Neisseria gonorrhoeae* is necessary for iron uptake from transferrin in the human host and requires the participation of two distinct proteins: TbpA and TbpB. TbpA is a TonB-dependent outer membrane transporter responsible for the transport of iron into the cell. TbpB is a lipid-modified protein, for which a precise role in receptor function has not yet been elucidated. These receptor complex proteins show promise as vaccine candidates; therefore, it is important to identify surface-exposed regions of the proteins required for wild-type functions. In this study we examined TbpB, which has been reported to be surface exposed in its entirety; however, this hypothesis has never been tested experimentally. We placed the hemagglutinin (HA) epitope into TbpB with the dual purpose of examining the surface exposure of particular epitopes as well as their impact on receptor function. Nine insertion mutants were created, placing the epitope downstream of the signal peptidase II cleavage site. We report that the HA epitope is surface accessible in all mutants, indicating that the full-length TbpB is completely surface exposed. By expressing the TbpB-HA fusion proteins in *N. gonorrhoeae*, we were able to examine the impact of each insertion on the function of TbpB and the transferrin acquisition process. We propose that TbpB is comprised of two transferrin-binding-competent lobes, both of which are critical for efficient iron uptake from human transferrin.

With the exception of a few species, most microorganisms require iron as an essential nutrient for growth and metabolic processes, including RNA synthesis and electron transport (8). The human host represents an extremely iron-limiting environment, with concentrations of soluble ferric iron rarely exceeding 10^{-18} M in tissue (46). In this environment, bacterial pathogens have evolved methods to overcome iron sequestration, which allows for replication and disease initiation. Many microorganisms produce siderophores in order to scavenge iron from their environment (30), while some have the ability to sequester host iron binding proteins in order to satisfy their growth requirements (3, 18, 28).

Neisseria gonorrhoeae, like the closely related obligate human pathogen *Neisseria meningitidis*, has not been shown to produce siderophores (2, 47). Instead, neisserial pathogens are capable of exploiting as iron sources host iron binding proteins such as human transferrin (hTf), human lactoferrin, and hemoglobin. The Tf iron acquisition system has been studied extensively in several human and veterinary pathogens (6, 17, 39, 41). In *N. gonorrhoeae*, expression of the Tf receptor is necessary to initiate an infection in human males (15), and its components show promise as vaccine candidates (11, 32).

Two distinct Tf-binding proteins, TbpA and TbpB, comprise the Tf iron internalization system; each protein specifically and independently binds hTf. TbpA, a TonB-dependent outer membrane transporter, is a necessary component of the Tf iron acquisition system and is responsible for transporting iron into the cell. TbpB is a putatively surface-exposed lipoprotein for which a precise role in Tf iron acquisition has not been defined. Although not required for iron internalization, TbpB makes the process more efficient (1). Unlike TbpA, TbpB has the ability to distinguish between apo- and holo-Tf, enhancing the interaction between the cell surface and the ferrated Tf molecule. This has led to the suggestion that the increased efficiency of iron uptake is due to TbpB's ability to select the optimum ligand for iron transport (16).

TbpB proteins are heterogeneous, exhibiting 69 to 84% sequence identity among *N. gonorrhoeae* strains and 64 to 75% identity when gonococcal TbpB proteins are compared to those of *N. meningitidis* (11). Regions of conservation have also been demonstrated between TbpB proteins of *N. gonorrhoeae*, *Actinobacillus pleuropneumoniae*, and *Moraxella catarrhalis*. Sequence analysis revealed conserved regions interspersed within hypervariable domains of TbpB (36, 38). Internal homology in the N- and C-terminal halves of TbpB has led to the suggestion that the protein adopts a bilobed structure similar to that of hTf (36). In *N. meningitidis* it was determined that both halves are able to bind Tf although the C terminus bound ligand with lower affinity (35).

Despite its heterogeneity, TbpB is an attractive vaccine candidate, since it is expressed by all clinical isolates and is not subject to high-frequency phase or antigenic variation (10, 28). Previous studies have also suggested that TbpB is surface exposed. Surface binding of Tf as well as bactericidal antibodies generated against the protein (16, 35) imply at least partial surface exposure; however, it is unclear exactly how much or what portions of TbpB are surface accessible. Therefore, determining what regions of the protein are readily surface accessible and/or involved in the protein's function would be

* Corresponding author. Mailing address: Department of Microbiology and Immunology, Virginia Commonwealth University Medical Center, P.O. Box 980678, Richmond, VA 23298-0678. Phone: (804) 827-1754. Fax: (804) 828-9946. E-mail: cncornel@vcu.edu.

▽ Published ahead of print on 16 April 2007.

advantageous for potential vaccine development. Computer prediction models of TbpB structure are inconclusive, offering no clear depiction of secondary protein structure (25; unpublished observations). Hydropathy plots reveal few hydrophobic domains typically seen in integral membrane proteins (unpublished observations). These data collectively suggest that TbpB is surface exposed and tethered to the outer membrane by its lipid moiety; however, no comprehensive test of this hypothesis has been attempted.

Although several functional analyses of TbpB have been accomplished, all involved the use of recombinant proteins (11, 24, 33–35, 37, 38). These studies have provided insight into in vitro Tf binding by TbpB but have stopped short of examining TbpB function in the native bacterium. In this study, we employed an epitope-tagging approach, which has been used to elucidate topological and functional characteristics of numerous proteins, including TbpA from *N. gonorrhoeae* (49) and FhuA from *Escherichia coli* (29). The hemagglutinin (HA) epitope was inserted at various positions in TbpB in order to probe surface accessibility in the gonococcal membrane and to examine the role of these targeted regions in Tf-iron internalization. The results from this analysis may have important implications in development of an efficacious TbpB-based vaccine.

MATERIALS AND METHODS

Strains and media. The strains utilized in this study are listed in Table 1. Gonococci were routinely grown on GC medium base (Difco), with Kellogg's supplement 1 (21) and 12 μM $Fe(NO_3)_3$. GC agar was supplemented with 100 μg/ml of streptomycin or 1 μg/ml of chloramphenicol for selection of gonococcal transformants. To achieve iron-stressed conditions, gonococci were grown in liquid chelexed defined medium (CDM) (48). All gonococcal strains were cultivated at 37°C in 5% CO_2. To assess Tf-iron utilization, CDM-agarose plates were supplemented with 30% saturated hTf (Sigma). One bacterial colony was streaked onto CDM-Tf plates and incubated for 24 to 48 h. Plasmids were propagated in *E. coli* strain TOP10 (Table 1), which was grown in Luria-Bertani broth supplemented with 50 μg/ml of kanamycin.

HA epitope insertion mutagenesis. Mutagenesis was carried out according to Horton et al. (19). The sequence encoding the HA epitope (YPYDVPDYA) was incorporated into *tbpB* via a two-step PCR technique, amplifying approximately 1 kb of *tbpB* from chromosomal DNA. Two primary PCRs were performed, each using an HA-encoding mutagenic primer as well as a gene-specific nonmutagenic primer (Table 2). The primary PCR products contained overlapping sequence encoding the HA epitope. These products were gel purified and used as a template for the secondary PCR. The second round of PCR was performed using two nonmutagenic primers (Table 2), with the overlapping region also serving to prime the reaction. The resulting secondary PCR product was gel purified, cloned, and sequenced. To create a negative control strain, a periplasmic protein (TonB) was also fused with the HA epitope. The *tonB* HA mutagenesis was performed in the manner described above.

Gonococcal transformation. Mutagenized *tbpB* products were subcloned into pHSS6-GCU (42), which contains the gonococcal DNA uptake sequence. TOPO pCR2.1 clones (Table 1) that contained portions of *tbpA* and *tonB* included native DNA uptake sequences, and thus these fragments were not subcloned into pHSS6-GCU. As described previously (49), a congression technique was employed to transform *N. gonorrhoeae* strain FA19 or FA6747 (Table 1) (49). Briefly, HA epitope encoding plasmid DNA was linearized and mixed with chromosomal DNA from MCV601 (Table 1). MCV601 contains an Ω cassette in the gene encoding *lbpB* (lactoferrin binding protein B) and therefore provides a marker for selecting transformed cells. Approximately 10 CFU was applied to a small area of a GC medium plate, and donor DNAs (HA-encoding and streptomycin-resistant [Str^r] DNA) were spotted on top of the piliated gonococci. Transformation mixtures were incubated on nonselective medium for 24 h at 37°C with 5% CO_2. Following incubation, single colonies were picked and restreaked on medium containing streptomycin. A PCR screen was employed on the Str^r transformants to detect the presence of the HA epitope sequence. When two mutations were combined, linearized plasmids containing each independent mutation were simultaneously added to piliated gonococci along with the Str^r chromosomal DNA.

Solid-phase Tf-binding assays. Gonococcal strains were grown under iron-stressed conditions as described above. After 4 h of growth, the cultures were standardized to culture density and applied to nitrocellulose. Membranes were allowed to dry and were then blocked in 5% skim milk in low-salt Tris-buffered saline (LS TBS). For assessment of solid-phase Tf binding, membranes were then incubated for 1 h with horseradish peroxidase-conjugated Tf (HRP-Tf) (Jackson ImmunoResearch), washed in LS TBS, and developed with Opti4-CN (Bio-Rad). Ligand discrimination and species specificity were assessed essentially as described previously (13). Membranes were probed with a mixture of unlabeled competitor (100% saturated hTf or apo-Tf) and HRP-Tf. To assess species specificity, membranes were probed with a mixture of unlabeled competitor (100% saturated hTf, bovine Tf, or murine Tf) and HRP-Tf. In both discrimination and species specificity assays, each well contained 0.33 μg of the HRP-Tf (commercially available HRP-Tf is partially saturated with iron). Twofold serial dilutions of unlabeled competitor (ranging from 6 μM to 0.05 μM) were made in the presence of 0.8 mM Desferal (Sigma) to prevent iron transfer. After the probing step, the nitrocellulose filter was washed in LS TBS and developed with Opti4-CN (Bio-Rad).

Western blotting for protein detection. Cultures were grown under iron-stressed conditions as described above. After 4 h of growth, cultures were standardized to culture density. Cells were pelleted and lysed with Laemmli solubilizing buffer. Five percent β-mercaptoethanol was added, and samples were boiled for 2 min. Samples underwent centrifugation for 2 min at 13,000 rpm and were then subjected to sodium dodecyl sulfate-polyacrylamide electrophoresis (23). Proteins were transferred to nitrocellulose membrane (Schleicher and Schuell) in 20 mM Tris base, 150 mM glycine, and 20% methanol in a submerged transfer apparatus (Bio-Rad). To detect the presence of the HA epitope, membranes were blocked in Western blocking reagent (Roche Molecular Biosciences) and probed with anti-HA peroxidase high-affinity (3F10) monoclonal antibody (Roche Molecular Biosciences). Membranes were developed using Perkin Elmer Chemiluminescence Plus (Perkin Elmer), and reactive bands were detected by exposure to film. To detect TbpB, membranes were blocked with 5% skim milk and incubated with polyclonal anti-TbpB antibody against *N. gonorrhoeae* strain FA1090 (31, 44). Alternatively, to detect Tf-binding by TbpB, membranes were probed with HRP-Tf as described previously (16). HRP was detected by Perkin Elmer Chemiluminescence Plus (Perkin Elmer), and reactive bands were identified by exposure to film. Detection of TbpA was accomplished using a polyclonal antibody to TbpA as described previously (16).

Confocal microscopy for surface-exposed HA epitope detection. To detect the presence of the HA epitope on the surface of gonococci, strains were grown under iron-stressed conditions. After 4 h of growth, the cultures were standardized to culture density and spotted onto glass slides. Slides were blocked in phosphate-buffered saline containing 0.1% immunoglobulin G-free bovine serum albumin and probed with 100 ng/ml anti-HA high-affinity (3F10) rat monoclonal antibody (Roche Molecular Biosciences). Slides were washed with 0.05% Tween-20 in phosphate-buffered saline and incubated with 1 μg/ml of Alexa 488-conjugated secondary antibody (Molecular Probes). Cells were visualized with a Zeiss LSM 510 Meta confocal imaging microscope.

Iron uptake assays. The iron uptake assay was performed essentially as described previously (1, 5, 12). hTf (CalBiochem) was 20% saturated with ^{55}Fe (Perkin Elmer). Strains were grown under iron-stressed conditions. After 3 h of growth, approximately 1.0×10^8 cells were added to each well of a Millipore multiscreen microtiter plate. KCN (40 μM) was added to one set of cultures to detect nonspecific iron binding to the cell surface. Approximately a 0.8 μM concentration of 20% saturated hTf (CalBiochem) was added to each well and incubated for 30 min to allow iron internalization. To stop the internalization reaction, plates were filtered. Each well was washed, dried, removed from the plate, and counted using a Beckman LS6500 beta counter. Counts were averaged, and the counts from the cultures with KCN were subtracted. Strains were standardized to total cellular protein, as determined by bicinchoninic acid assay (Pierce). Each graph is a representation of data from three separate assays, each performed in triplicate.

Statistical analysis. Statistical significance of iron internalization was determined using a two-tailed paired Student's *t* test in which a P value of ≤ 0.05 was considered significant.

RESULTS

Alignment of TbpB proteins from bacterial pathogens and rationale for choice of HA insertion locations. While it has

TABLE 1. Strains and plasmids used in the current study

Strain or plasmid	Phenotype (genotype)[a]	Reference or source
E. coli TOP10	F$^-$ *mcrA* Δ(*mrr-hsdRMS-mcrBC*) Φ80*lacZ*Δ*M15* Δ*lacX74 recA1 deoR araD139* Δ(*ara-leu*) 7697 *galU galK rpsL* (Str^r) *endA1 nupG*	Invitrogen
N. gonorrhoeae strains		
FA19	Wild type	28
FA6747	TbpA$^-$ (*tbpA*::mTn*3*cat)	14
FA6905	TbpB$^-$ (Δ*tbpB*)	16
FA6815	TbpA$^-$ TbpB$^-$ (*tbpB*::Ω)	1
MCV515	L9HA TbpA Lbp$^-$ (*tbpA*∇HA *lbp*::Ω)	49
MCV516	L9HA TbpA Lbp$^-$(*tbpA*∇HA Δ*tbpB lbp*::Ω)	49
MCV601	FA19; Lbp$^-$ (*lbp*::Ω)	22
MCV801	HA1$_{(37)}$ TbpB Lbp$^-$ (*tbpB*∇HA *lbp*::Ω)	This study
MCV802	HA2$_{(97)}$ TbpB TbpA$^-$ Lbp$^-$ (*tbpB*∇HA *lbp*::Ω)	This study
MCV803	HA1$_{(37)}$ TbpB Lbp$^-$ (*tbpB*∇HA *tbpA*::mTn*3 lbp*::Ω)	This study
MCV804	HA2$_{(97)}$ TbpB TbpA$^-$ Lbp$^-$ (*tbpB*∇HA *tbpA*::mTn*3 lbp*::Ω)	This study
MCV812	HA3$_{(175)}$ TbpB Lbp$^-$ (*tbpB*∇HA *lbp*::Ω)	This study
MCV813	HA3$_{(175)}$ TbpB TbpA$^-$ Lbp$^-$ (*tbpB*∇HA *tbpA*::mTn*3 lbp*::Ω)	This study
MCV814	HA4$_{(293)}$ TbpB Lbp$^-$ (*tbpB*∇HA *lbp*::Ω)	This study
MCV815	HA4$_{(293)}$ TbpB TbpA$^-$ Lbp$^-$ (*tbpB*∇HA *tbpA*::mTn*3 lbp*::Ω)	This study
MCV816	HA5$_{(327)}$ TbpB Lbp$^-$ (*tbpB*∇HA *lbp*::Ω)	This study
MCV817	HA5$_{(327)}$ TbpB TbpA$^-$ Lbp$^-$ (*tbpB*∇HA *tbpA*::*mTn3 lbp*::Ω)	This study
MCV818	HA6$_{(424)}$ TbpB Lbp$^-$ (*tbpB*∇HA *lbp*::Ω)	This study
MCV819	HA6$_{(424)}$ TbpB TbpA$^-$ Lbp$^-$ (*tbpB*∇HA *tbpA*::mTn*3 lbp*::Ω)	This study
MCV820	HA7$_{(453)}$ TbpB Lbp$^-$ (*tbpB*∇HA, *lbp*::Ω)	This study
MCV821	HA7$_{(453)}$ TbpB TbpA$^-$ Lbp$^-$ (*tbpB*∇HA *tbpA*::mTn*3 lbp*::Ω)	This study
MCV822	HA8$_{(607)}$ TbpB Lbp$^-$ (*tbpB*∇HA *lbp*::Ω)	This study
MCV823	HA8$_{(607)}$ TbpB TbpA$^-$ Lbp$^-$ (*tbpB*∇HA *tbpA*::mTn*3 lbp*::Ω)	This study
MCV824	HA9$_{(660)}$ TbpB Lbp$^-$ (*tbpB*∇HA *lbp*::Ω)	This study
MCV825	HA9$_{(660)}$ TbpB TbpA$^-$ Lbp$^-$ (*tbpB*∇HA *tbpA*::mTn*3 lbp*::Ω)	This study
MCV826	HA1$_{(37)}$ TbpB L9HA TbpA Lbp$^-$ (*tbpB*∇HA *tbpA*∇HA *lbp*::Ω)	This study
MCV827	HA2$_{(97)}$ TbpB L9HA TbpA Lbp$^-$ (*tbpB*∇HA *tbpA*∇HA *lbp*::Ω)	This study
MCV828	HA3$_{(175)}$ TbpB L9HA TbpA Lbp$^-$ (*tbpB*∇HA *tbpA*∇HA *lbp*::Ω)	This study
MCV829	HA4$_{(293)}$ TbpB L9HA TbpA Lbp$^-$ (*tbpB*∇HA *tbpA*∇HA *lbp*::Ω)	This study
MCV830	HA5$_{(328)}$ TbpB L9HA TbpA Lbp$^-$ (*tbpB*∇HA *tbpA*∇HA *lbp*::Ω)	This study
MCV831	HA6$_{(424)}$ TbpB L9HA TbpA Lbp$^-$ (*tbpB*∇HA *tbpA*∇HA *lbp*::Ω)	This study
MCV832	HA7$_{(453)}$ TbpB L9HA TbpA Lbp$^-$ (*tbpB*∇HA *tbpA*∇HA *lbp*::Ω)	This study
MCV833	HA8$_{(607)}$ TbpB L9HA TbpA Lbp$^-$ (*tbpB*∇HA *tbpA*∇HA *lbp*::Ω)	This study
MCV834	HA9$_{(660)}$ TbpB L9HA TbpA Lbp$^-$ (*tbpB*∇HA *tbpA*∇HA *lbp*::Ω)	This study
MCV836	HA5$_{(328)}$ HA7$_{(453)}$ TbpB TbpA$^-$ Lbp$^-$ (*tbpB*∇HA *tbpA*::mTn*3 lbp*::Ω)	This study
MCV838	HA5$_{(328)}$ HA9$_{(660)}$ TbpB TbpA$^-$ Lbp$^-$ (*tbpB*∇HA, *tbpA*::mTn*3 lbp*::Ω)	This study
MCV847	TonBHA$_{(160)}$ Lbp$^-$ (*tonB*∇HA *lbp*::Ω)	This study
MCV848	HA4$_{(293)}$ HA8$_{(607)}$ TbpB TbpA$^-$ Lbp$^-$ (*tbpB*∇HA *tbpA*::mTn*3 lbp*::Ω)	This study
MCV849	HA5$_{(328)}$ HA8$_{(607)}$ TbpB TbpA$^-$ Lbp$^-$ (*tbpB*∇HA *tbpA*::mTn*3 lbp*::Ω)	This study
Plasmids		
pCR2.1	Kan^r Amp^r	Invitrogen
pHSS6GCU	Vector containing gonococcal uptake sequence (Kan^r)	42
pVCU521	pCR2.1 containing *tbpA* gene fragment; HA in L9	49
pVCU690	pCR2.1 containing *tonB*(Δ160–194)	22
pVCU801	pCR2.1 containing *tbpB* gene fragment amplified by PCR with primers oVCU136 and oVCU141; HA1	This study
pVCU802	pCR2.1 containing *tbpB* gene fragment amplified by PCR with primers oVCU136 and oVCU141; HA2	This study
pVCU803	pHSS6GCU containing EcoRI fragment from pVCU801	This study
pVCU804	pHSS6GCU containing EcoRI fragment from pVCU802	This study
pVCU813	pCR2.1 containing *tbpB* gene fragment amplified by PCR with primers GC553 and oVCU216; HA3	This study
pVCU814	pHSS6GCU containing EcoRI fragment from pVCU813	This study
pVCU815	pCR2.1 containing *tbpB* gene fragment amplified by PCR with primers GC555 and oVCU219; HA4	This study
pVCU816	pHSS6GCU containing EcoRI fragment from pVCU815	This study
pVCU817	pCR2.1 containing *tbpB* gene fragment amplified by PCR with primers GC555 and oVCU219; HA5	This study
pVCU818	pHSS6GCU containing EcoRI fragment from pVCU817	This study
pVCU819	pCR2.1 containing *tbpB* gene fragment amplified by PCR with primers GC561 and oVCU226; HA6	This study
pVCU820	pHSS6GCU containing EcoRI fragment from pVCU819	This study
pVCU821	pCR2.1 containing *tbpB* gene fragment amplified by PCR with primers GC561 and oVCU226; HA7	This study
pVCU822	pHSS6GCU containing EcoRI fragment from pVCU821	This study
pVCU823	pCR2.1 containing *tbpB* gene fragment amplified by PCR with primers GC561 and oVCU226; HA8	This study
pVCU824	pHSS6GCU containing EcoRI fragment from pVCU822	This study
pVCU825	pCR2.1 containing *tbpB* gene fragment amplified by PCR with primers GC556 and Tfbp12; HA9	This study
pVCU826	pHSS6GCU containing EcoRI fragment from pVCU825	This study
pVCU836	pCR2.1 containing *tonB* gene amplified by PCR with primers oVCU142 and oVCU143; TonBHA	This study

[a] Phenotype listed includes position of the last amino acid prior to HA insertion (parentheses). Residues are numbered starting from the first amino acid in the mature protein. ∇, insertion of the HA epitope.

been proposed that TbpB is entirely surface exposed, this hypothesis has not been tested experimentally in *N. gonorrhoeae*. To accomplish this task, TbpB-HA fusion proteins were created by inserting sequence encoding the HA epitope into the *tbpB* gene. TbpB proteins are heterogeneous and consist of hypervariable domains interspersed with regions of conservation. Figure 1 represents an alignment of TbpB proteins from *N. gonorrhoeae*, *N. meningitidis*, *M. catarrhalis*, and *A. pleuropneumoniae*. The alignment depicts the previously identified N-terminal domains necessary for Tf binding by *N. gonorrhoeae*

TABLE 2. Primers used in this study

Primer	Sequence (5′–3′)[a]	Amplification target (HA epitope)
GC553	ATTGCCGACAGAACCCA	*tbpB*
GC555	AAGCACGAGGGTTATGG	*tbpB*
GC556	CACCGCAAATGGCAATG	*tbpB*
GC561	CTTCTTTGAGCGGCGGC	*tbpB*
Tfbp-12	GGCATAAAATATTTAATCGGA	*tbpA*
oVCU136	ATGAACAATCCATTGGTGAATC	*tbpB*
oVCU137	GTCCGGGACGTCGTACGGGTAGTCTTTTCGGGCTTCCGG	*tbpB* (HA1)
oVCU138	CCGTACGACGTCCCGGACTACGCCCAAGGCGGATACGGTTTTGC	*tbpB* (HA1)
oVCU139	GTCCGGGACGTCGTACGGGTA ACCGTTGGTTTCTACTTCTG	*tbpB* (HA2)
oVCU140	CCGTACGACGTCCCGGACTACGCCAATTCTAAAATGTACACTTCACCT	*tbpB* (HA2)
oVCU141	GCCGCCGCTCAAAGAAGAC	*tbpB*
oVCU142	GCCTATGAATGGAGCAGGC	*tonB*
oVCU143	GTCCTGCCCTAGCGGGC	*tonB*
oVCU208	GTCCGGGACGTCGTACGGGTATTGTCGGGAAGGTTTGTCG	*tbpB* (HA3)
oVCU209	CCGTACGACGTCCCGGACTACGCCCTTCCCGCTTCTGAAGCAG	*tbpB* (HA3)
oVCU210	GTCCGGGACGTCGTACGGGTACTTGCCGCTGAAGCGGTT	*tbpB* (HA4)
oVCU211	CCGTACGACGTCCCGGACTACGCCGCGATAGCGACCGACAAAC	*tbpB* (HA4)
oVCU212	GTCCGGGACGTCGTACGGGTACTCACCCTGCGGGCCGAA	*tbpB* (HA5)
oVCU213	CCGTACGACGTCCCGGACTACGCCGAATTGGGTTTCCGCTTTTTG	*tbpB* (HA5)
oVCU214	GTCCGGGACGTCGTACGGGTATTTATCTGCCTGACCGTTCC	*tbpB* (HA6)
oVCU215	CCGTACGACGTCCCGGACTACGCCGGTAAAAACGGCGGAACAGA	*tbpB* (HA6)
oVCU216	CGGGCTGTAGGTTGTTTCG	*tbpB*
oVCU217	GTCCGGGACGTCGTACGGGTACGCGCCTGTTTGGGCTTT	*tbpB* (HA7)
oVCU218	CCGTACGACGTCCCGGACTACGCCGGCGGCATGCAAACCGCT	*tbpB* (HA7)
oVCU219	CTCAATCATGGCGTCAATGG	*tbpB*
oVCU220	GTCCGGGACGTCGTACGGGTACGTACCTTTAAAGCCGTTGC	*tbpB* (HA8)
oVCU221	CCGTACGACGTCCCGGACTACGCCGCGAAAACCGGTAATGACGG	*tbpB* (HA8)
oVCU224	GTCCGGGACGTCGTACGGGTATTTCGTTTGTTCATTGCCCG	*tbpB* (HA9)
oVCU225	CCGTACGACGTCCCGGACTACGCCAATGCAACAGTTGAATCCGG	*tbpB* (HA9)
oVCU226	CACAAGCTTTTGGCGTTTCGC	*tbpB*
oVCU327	CCGTACGACGTCCCGGACTACGCCACCGGTGTCGGCAGCAGC	*tonB*
oVCU328	GTCCGGGACGTCGTACGGGTATCCCTTACCTTCCCCATTACC	*tonB*

[a] Sequences encoding the HA epitope are underlined.

(11) and *N. meningitidis* (45). Ligand binding by the N-terminal half of TbpB is resistant to denaturation and can be detected by Western blotting. Therefore, these domains represent the largest N-terminal portion of the protein required for Tf binding by Western blotting. The regions previously determined to be important for solid-phase Tf binding by *N. meningitidis* TbpB (35) are also noted in the alignment (Fig. 1). The full-length mature protein was targeted for mutagenesis in the current study; we placed the HA epitope at various positions downstream of the signal II peptidase cleavage site (LSAC) (Fig. 1). We divided the protein into N- and C-terminal halves based on the limits of the N-terminal binding domain (Fig. 1) and assessed the relative contributions of each TbpB half to protein function. Locations of the HA epitope insertions are indicated by numbers 1 to 9. We chose nine regions of TbpB for HA epitope insertion, targeting areas of sequence variability as well as conserved regions. We reasoned that areas of sequence diversity would accommodate the insertion, causing minimal disruption to the mature protein. HA insertion 3 (HA3) was placed within a domain homologous to one in *A. pleuropneumoniae* found to bind Tf (43). Five conserved regions were identified in both the N- and C-terminal halves of TbpB (boxed in Fig. 1). Regions N1 through N5 are located in the N-terminal half; regions C1 through C5 are homologous and located within the C-terminal half. HA insertions 4 and 8 targeted the homologous regions N3 and C3, respectively, while insertion 5 was placed within a highly conserved domain, N4 (Fig. 1). The region targeted by HA4 was also located within a previously identified (35) N-terminal Tf-binding domain of *N. meningitidis* (Fig. 1). All of the HA fusion proteins were expressed in *N. gonorrhoeae* strain FA19 (Table 1) with the intent of examining surface exposure of TbpB and structure-function relationships in the protein.

TbpB is entirely surface exposed. Utilizing a polyclonal anti-TbpB serum, we determined that the TbpB-HA fusions were surface exposed in all mutants as analyzed by both solid-phase antibody binding assay and immunofluorescence microscopy (data not shown). A negative control strain (TonB-HA) was created by fusing a periplasmic protein (TonB) with the HA epitope (Table 1). This negative control strain was used for surface exposure experiments. Visualization of cells by microscopy revealed that the gonococcal cells were intact (Fig. 2). An immunofluorescence assay performed with an anti-HA monoclonal antibody indicated that the HA epitope was surface exposed in all strains except the TonB-HA fusion negative control strain. The various degrees of reactivity with the monoclonal antibody were most likely due to structural constraints and/or surrounding protein sequence. These trends were confirmed by solid-phase whole-cell HA-antibody binding experiments (data not shown). Since TbpB and TbpA have been shown to function together, potentially interacting within the outer membrane (7, 20, 22), we examined HA surface exposure

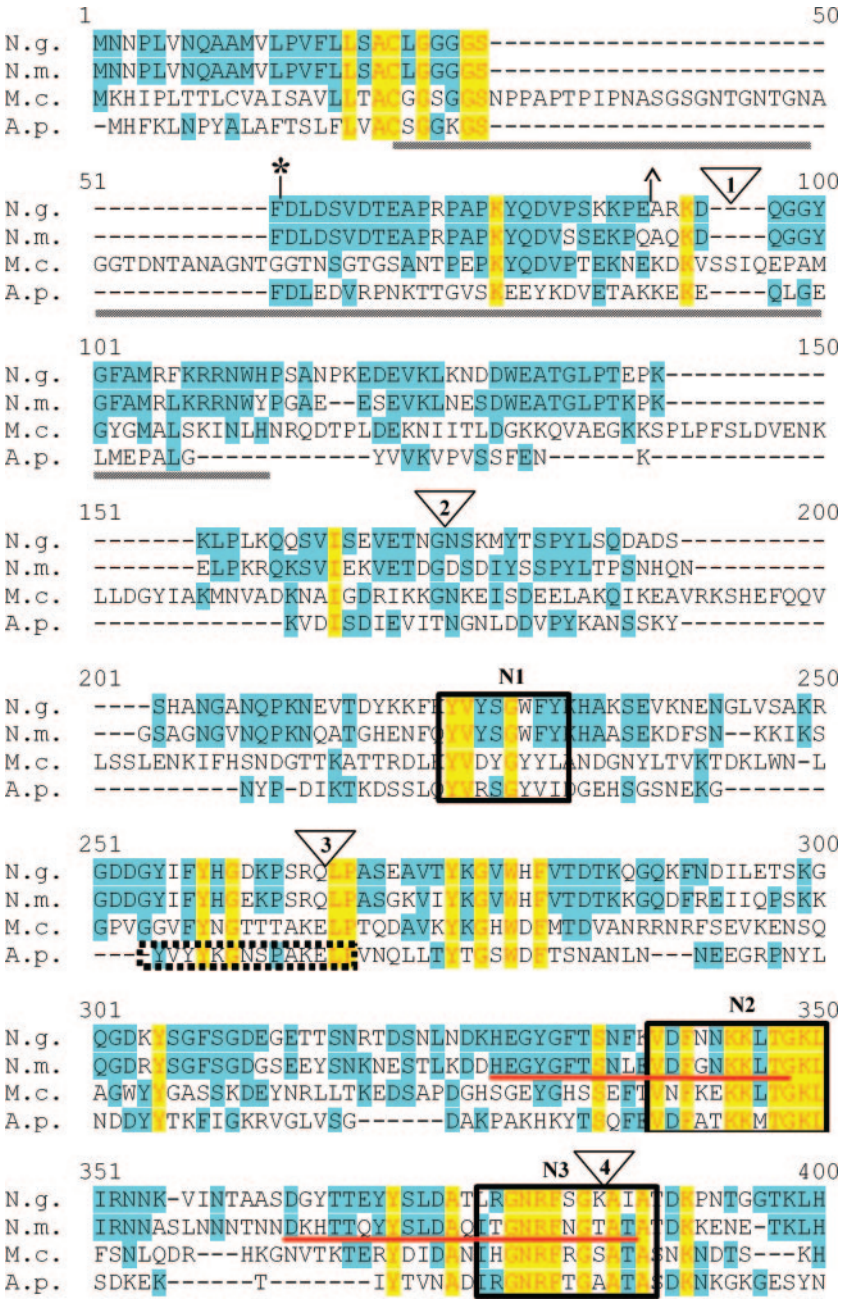

FIG. 1. Alignment of TbpB proteins from bacterial pathogens. TbpB from *N. gonorrhoeae* FA19 (N.g.), *N. meningitidis* M982 (N.m.), *M. catarrhalis* 4223 (M.c.), and *A. pleuropneumoniae* serotype 7 (A.p.) were aligned with the program Vector NTI. Identical residues are shaded in yellow while similar residues are shaded in blue. HA epitope fusion points are shown as triangles numbered 1 to 9. Previously identified regions of conservation among TbpB proteins are underlined by gray lines (11). The previously identified denaturation-resistant Tf-binding domains in the TbpB proteins of *N. gonorrhoeae* (*) and *N. meningitidis* (^) are flanked by their respective symbols. The double arrowhead indicates the division between the N- and C-terminal halves of the protein. Regions of internal similarity between the N- and C-terminal halves of TbpB are boxed and labeled N1 through N5 and C1 through C5, respectively. The sequence motifs previously identified as important for high-affinity Tf binding of *N. meningitidis* (35) are underlined in red. The *A. pleuropneumoniae* peptide shown to bind Tf (43) is denoted by the dotted-line box.

by immunofluorescence microscopy in both the presence and absence of TbpA. No detectable differences in the surface exposure of TbpB epitopes were seen, regardless of the presence of TbpA (data not shown).

HA epitope insertions define 35 critical residues for Tf binding by Western blotting. Western blot analysis of HA fusion strains indicated that the 86-kDa full-length TbpB was expressed (Fig. 3A) and that the HA epitope could be detected in the full-length protein (Fig. 3B). Multiple species were present in both the anti-TbpB and anti-HA Western blots, possibly indicating that TbpB assumes multiple conformational forms persisting under denaturing conditions. Noteworthy is

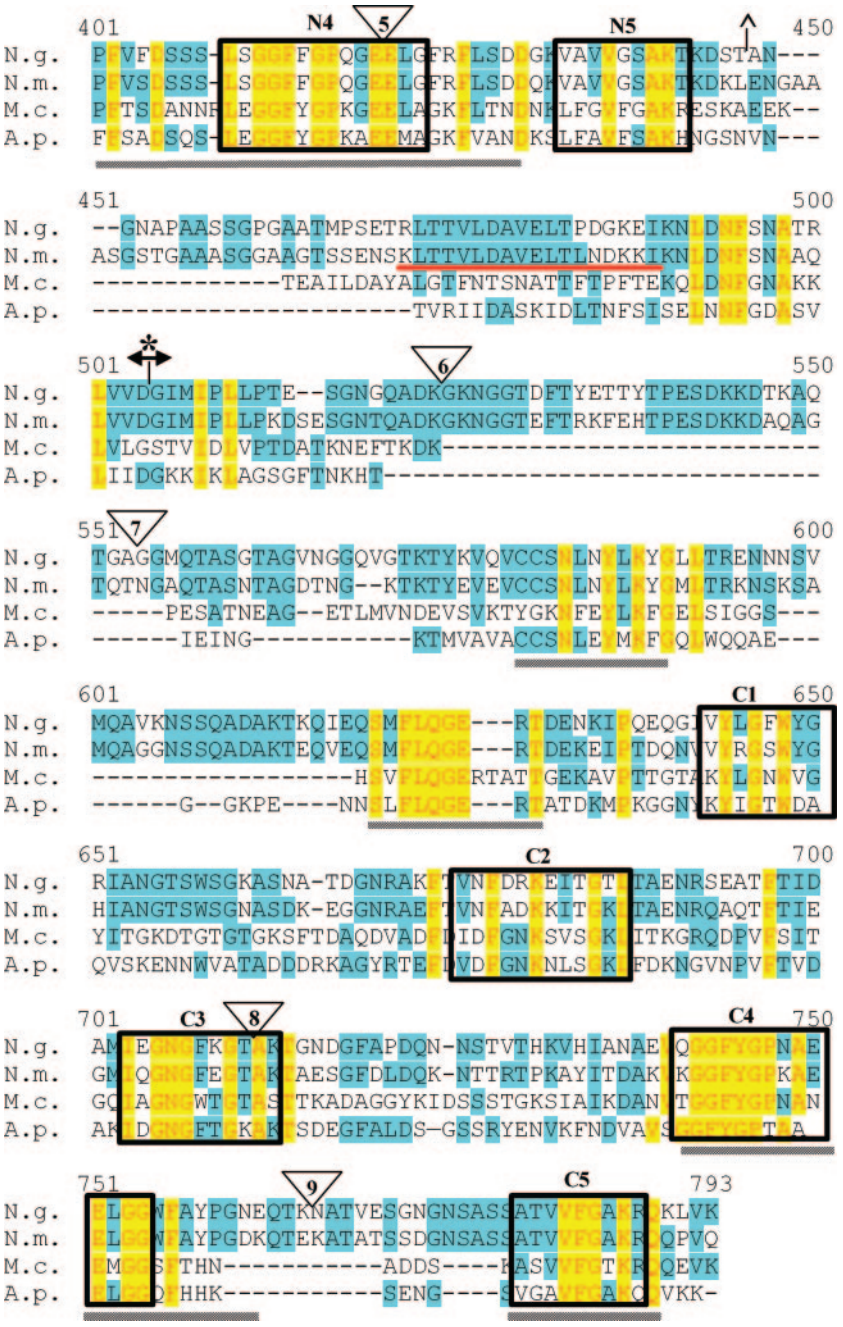

FIG. 1—*Continued.*

the inability to detect these other TbpB species in the HA1 insertion strains by anti-HA Western blotting (Fig. 3B), suggesting the possibility that these alternate species were N-terminally truncated between the insertion points of HA1 and HA2. These other forms of TbpB were also seen in the wild-type control strain (Fig. 3A); thus, they did not result from TbpB mutagenesis. It was shown previously by Western blotting that a high-affinity Tf-binding domain, comprising the amino-terminal half of TbpB, is resistant to denaturation and responsible for Tf binding (11). Strains expressing insertions 1 to 5 contain the HA epitope within this denaturation-resistant, high-affinity binding domain. Tf binding by TbpB assessed under denaturing conditions revealed that binding was either diminished (HA3) or abolished (HA4 and HA5) in a subset of these mutants (Fig. 3C). Although insertions 1 to 5 were all located within the high-affinity Tf-binding domain, only those located between residues 293 and 328 (insertions 4 and 5) resulted in the most pronounced phenotypes. This 35-residue region, defined by insertions 4 and 5, is therefore critical in wild-type TbpB binding function.

Three HA epitope insertions impair Tf binding to the gonococcal surface. Solid-phase binding assays utilizing HRP-Tf

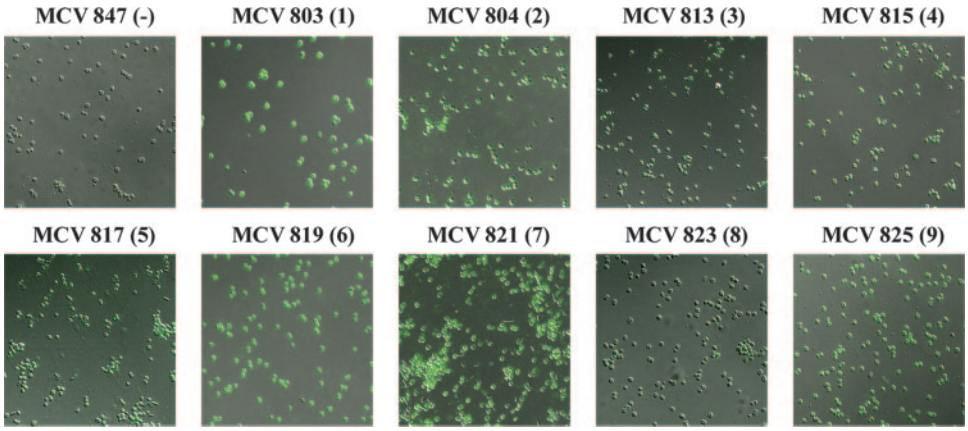

FIG. 2. Immunofluorescence microscopy of TbpB-HA fusion strains. Iron-stressed gonococci were applied to glass slides and probed with an anti-HA monoclonal antibody followed by an Alexa 488-conjugated secondary antibody. Cells were visualized with a Zeiss LSM 510 Meta confocal microscope, at a magnification of ×63. Each image is labeled according to strain name with the HA epitope insertion number in parentheses. All TbpB-HA fusion strains are shown in a TbpA$^-$ background. MCV847 (TonB-HA fusion) serves as the negative control.

were performed to assess the impact of each HA epitope on TbpB's surface-deployed ligand binding function. Since both TbpA and TbpB independently bind Tf, specific ligand binding by TbpB can only be assessed in the absence of TbpA. HA insertion strains 4, 5, and 8 demonstrated decreased surface Tf binding in the TbpA$^-$ background (Fig. 4). HA fusion mutants 4 and 5 contained insertions within the N-terminal Tf-binding domain and did not bind Tf, as assessed by Western blotting (Fig. 3C). The HA8 insertion was located in the C-terminal half of TbpB and exhibited decreased surface binding. These data suggest the presence of a functional Tf-binding domain within the C-terminal half of TbpB, even though its presence was not detectable by Western blotting approaches. Disruption of duplicated regions N3 and C3 (targeted by HA4 and HA8, respectively) caused a similarly diminished surface Tf-binding capacity. Taken together, these data suggest that the duplicated regions within the N and C termini of TbpB are associated with two distinct Tf-binding domains.

Specific binding of ferrated ligand is not sufficient to enhance iron uptake. TbpB is not necessary for uptake of iron; however, iron internalization from Tf is more efficient in the presence of TbpB (1). It was previously shown that TbpB, unlike TbpA, has the ability to discriminate between ferrated and apo-Tf, preferentially binding ferrated Tf (16). These findings cumulatively suggest that TbpB enhances iron uptake due to its ability to select the optimum ligand. Utilizing the TbpB-HA fusion strains, we examined ligand discrimination, species specificity, and iron internalization. In order to assess ligand discrimination, a solid-phase competition assay was performed (Fig. 5). Strains were incubated with HRP-Tf (partially

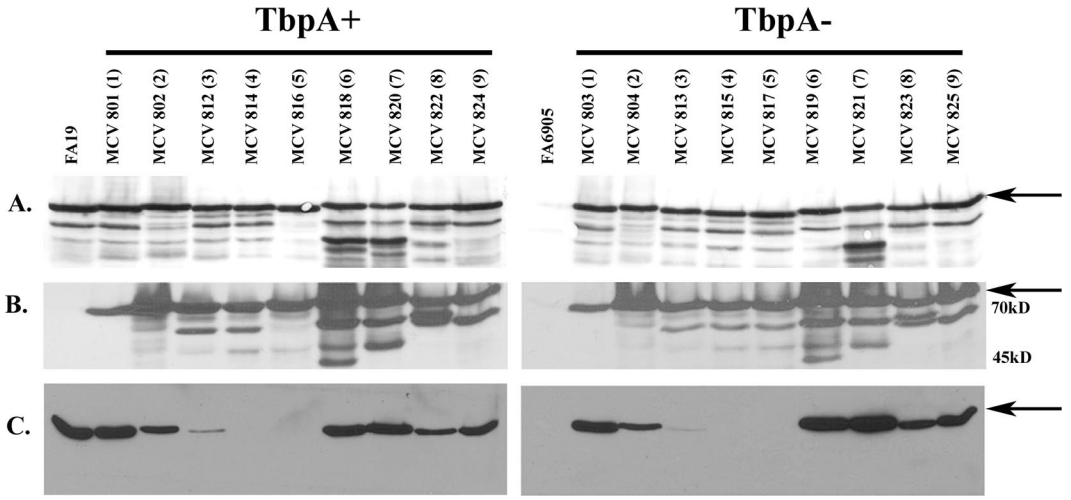

FIG. 3. Expression of TbpB-HA fusion proteins. Iron-stressed gonococci were lysed, subjected to sodium dodecyl sulfate-polyacrylamide electrophoresis, and following transfer to nitrocellulose, probed with one of the following antibodies: polyclonal anti-TbpB serum (A) or peroxidase-conjugated high-affinity HA-specific antibody (B). Tf binding by the fusion proteins was assessed by probing with peroxidase-conjugated hTf (C). For both TbpA-expressing (+) and -nonexpressing (−) strains, each lane is labeled according to strain name with the HA epitope insertion number in parentheses. The arrows indicate the position of full-length TbpB (approximately 86 kDa). The positions of molecular mass markers are indicated on the right. FA19 and FA6905 serve as the wild-type and TbpB$^-$ controls, respectively.

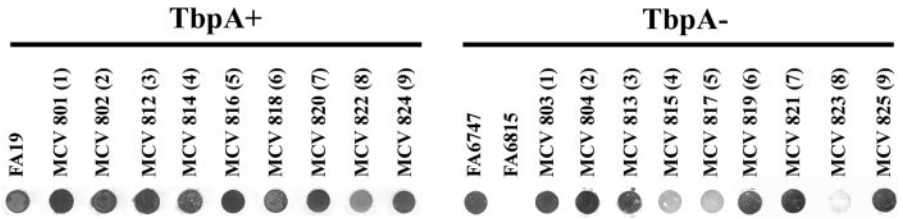

FIG. 4. Solid-phase Tf-binding assay of whole gonococci. Iron-stressed whole gonococci were applied to nitrocellulose, and Tf binding was examined by probing with peroxidase-conjugated hTf. For both TbpA-expressing (+) and -nonexpressing (−) strains, each lane is labeled according to strain name with the HA epitope insertion number in parentheses. FA19 and FA6815 (TbpA$^-$ TbpB$^-$) serve as the wild-type and negative controls, respectively. FA6747 serves as the TbpA$^-$ control.

saturated) in mixtures with either ferrated Tf or apo-Tf as competitor. As shown in Fig. 5, all of the HA fusion mutants retained their ability to preferentially bind ferrated Tf. Differences in total binding were detected, supporting the results of the solid-phase Tf-binding assay (Fig. 4). It is possible that there are multiple domains necessary for ligand discrimination or that we have not targeted the specific region responsible for this function.

The Tf receptors of *N. gonorrhoeae* and *N. meningitidis* are specific for hTf (40). It has been suggested previously that the N-terminal domain of meningococcal TbpB is responsible for species specificity (35). To assess whether we had impacted a domain necessary for species-specific binding by TbpB, we examined the ability of fusion strains HA4, HA5, and HA8 to bind bovine and murine Tf in a solid-phase competition assay. These strains demonstrated a defect in Tf binding (Fig. 4) and were chosen in order to examine whether this defect correlated with a decrease in species-specific Tf binding. Strains were incubated with mixtures of human HRP-Tf and either ferrated hTf, bovine Tf, or mu-

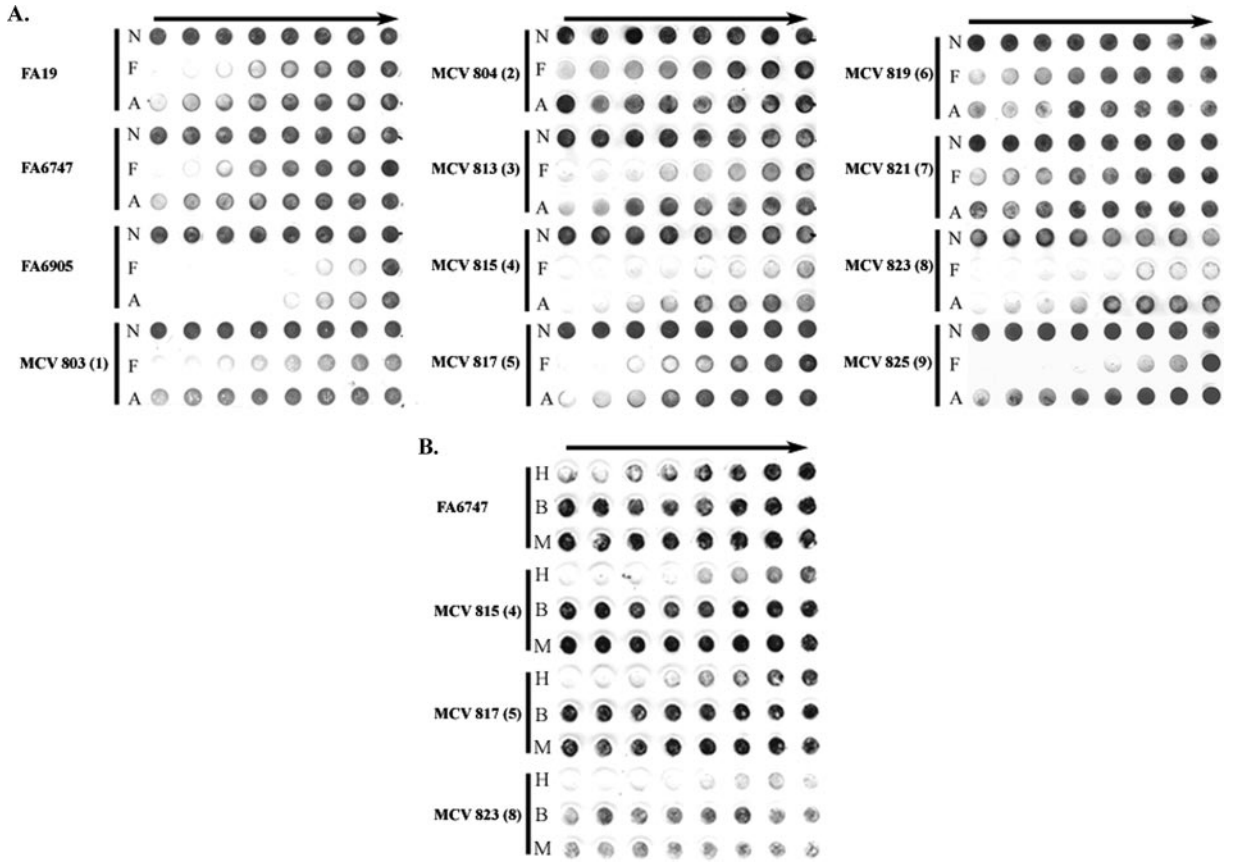

FIG. 5. Solid-phase Tf discrimination assays. Iron-stressed whole gonococci were applied to nitrocellulose, and the ability to discriminate between different forms of Tf was assessed. In panel A, cells were incubated with HRP-Tf and varying amounts of competitor: N, no competitor; F, ferrated Tf; or A, apo-Tf. In panel B, cells were incubated with HRP-Tf and varying amounts of competitor: H,hTf; B, bovine Tf; or M, murine Tf. Competitor concentration decreases from left to right (solid arrows). All mutant strains were tested for Tf-binding specificity in the absence of TbpA. Each series of three rows is labeled according to strain name with the HA epitope insertion number in parentheses. FA19 serves as the wild-type control. FA6747 and FA6905 are the TbpA$^-$ and TbpB$^-$ controls, respectively.

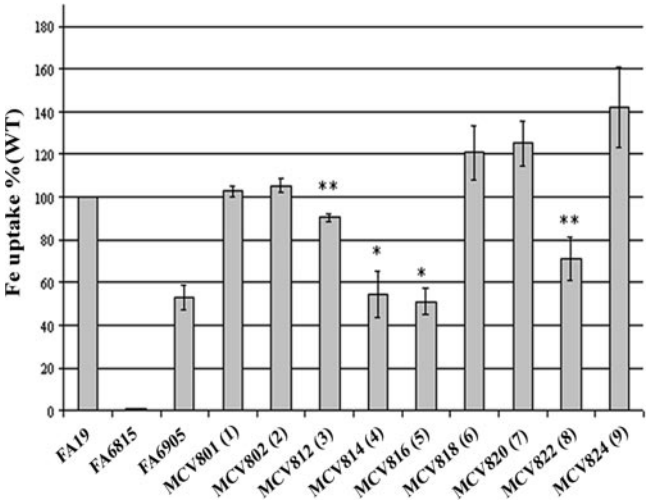

FIG. 6. ^{55}Fe uptake by TbpB-HA mutants. Iron-stressed gonococci were incubated with ^{55}Fe-labeled Tf. ^{55}Fe uptake was measured as a percentage of wild type. Each bar represents the mean of three independent experiments. Each bar is labeled according to strain name with the HA epitope insertion number in parentheses. FA19 and FA6815 (TbpA$^-$ TbpB$^-$) serve as the wild-type and negative controls, respectively. FA6905 serves as a TbpB$^-$ control strain. Standard deviations are represented by error bars. *, $P \leq 0.05$ in comparison to wild type; **, $P \leq 0.05$ in comparison to both wild type and FA6905.

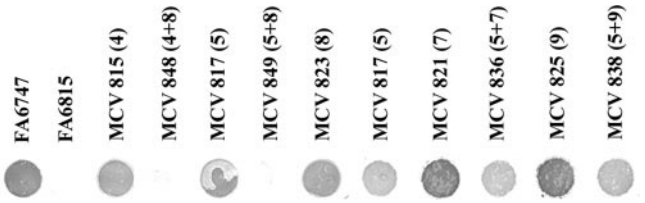

FIG. 7. Solid-phase Tf-binding assay of combination mutants. Iron-stressed whole gonococci were applied to nitrocellulose, and binding of Tf was examined by probing with peroxidase-conjugated hTf. Each column is labeled according to strain name with the HA epitope(s) insertion number in parentheses. FA6747 and FA6815 serve as the TbpB$^+$ and TbpB$^-$ control strains, respectively. All strains are TbpA$^-$.

rine Tf as competitor (Fig. 5B). All of the HA fusion strains preferentially bound hTf, indicating that the binding site that remained after mutagenesis was still specific for the human form of the ligand.

We also examined iron internalization utilizing ^{55}Fe-loaded Tf (Fig. 6). In this assay we compared total uptake by each mutant strain as a percentage of wild-type iron internalization. In the absence of both TbpB and TbpA (FA6815), iron internalization was abolished. In the absence of TbpB (FA6905), uptake of iron was approximately 50% of the wild-type level. In all mutants, TbpB and TbpA levels were similar to the wild-type level (Fig. 4A and data not shown), indicating that the altered amount of iron uptake was due to the presence of the HA in TbpB and not merely that more or less of the receptor proteins was present. HA1 and HA2 fusion strains internalized ^{55}Fe from Tf in a manner that was statistically indistinguishable from wild type. Fusion strain HA3, on the other hand, internalized less iron than wild type but more than the TbpB deletion mutant (FA6905). This decreased iron internalization by the HA3 fusion strain supports the diminished Tf binding determined by Western blotting (Fig. 3C). This analysis also demonstrated that the region defined by insertions 4 and 5 plays an important role in wild-type TbpB function. HA4 and HA5 fusion strains internalized ^{55}Fe from Tf in a manner that was statistically indistinguishable from the TbpB deletion strain (FA6905), implying that decreased Tf-binding results in decreased uptake of iron. The fusion strains HA6 ($P \leq 0.1$), HA7 ($P \leq 0.06$), and HA9 ($P \leq 0.06$) appeared to internalize somewhat higher levels of ^{55}Fe from Tf; however, these levels were statistically indistinguishable from the wild-type level. Finally, the HA8 fusion strain internalized less ^{55}Fe compared to wild type but more than the TbpB deletion mutant, consistent with the decreased Tf binding shown in Fig. 3 and 4. This observation supports the hypothesis that the duplicated regions targeted in fusion strains HA8 and HA4 perform similar functions in wild-type TbpB. However, it appears that the domain targeted in HA4 has a greater impact on the wild-type binding function than the C-terminal region disrupted in HA8. Overall, these results indicate that the ability to discriminate and preferentially bind the optimum ligand is not sufficient to enhance iron uptake from Tf. Moreover, it is evident that the loss of either surface Tf-binding site in TbpB is directly correlated with decreased efficiency of iron internalization.

Both N- and C-terminal halves of TbpB are necessary for surface binding of Tf. To assess whether other Tf-binding domains, in addition to those already disrupted, were present, we combined mutations in the N terminus of TbpB with HA8, which is localized in the C-terminal half (Table 1). Solid-phase binding assays were performed to examine Tf binding by TbpB in the combined fusion strains HA4+HA8 and HA5+HA8. We hypothesized that combining mutations in the independent Tf-binding domains would either abolish surface binding or reveal yet another unidentified ligand binding region. Figure 7 demonstrates surface Tf binding by the combined HA insertion mutants compared to the individual epitope insertion mutants. In the HA4+HA8 and HA5+HA8 combined mutants, Tf binding by TbpB was abolished, indicating that we had targeted all of the domains necessary for surface Tf binding by TbpB. We also created the combined mutants HA5+HA7 and HA5+HA9, with the hypothesis being that TbpB should maintain its ability to bind Tf since the C-terminal binding region had not been disrupted. The HA5+HA7 and HA5+HA9 combined fusion strains bound Tf in a manner similar to the parental strain (HA5 fusion) (Fig. 7). These results suggested that TbpB was not grossly impacted by the presence of two HA epitope insertions. These findings indicate that the N-terminal Tf-binding domain is interrupted by HA insertions 4 and 5, while insertion 8 interfered with the function of the C-terminal binding domain. Overall, these data suggest that wild-type surface Tf binding requires both the N- and C-terminal domains.

Both the N- and C-terminal halves of TbpB are required to compensate for a TbpA defect. In order to examine the impact of the HA insertions on the function of the TbpA/TbpB iron acquisition system, we utilized a previously created TbpA mutant (MCV515) that absolutely requires TbpB for Tf-iron ac-

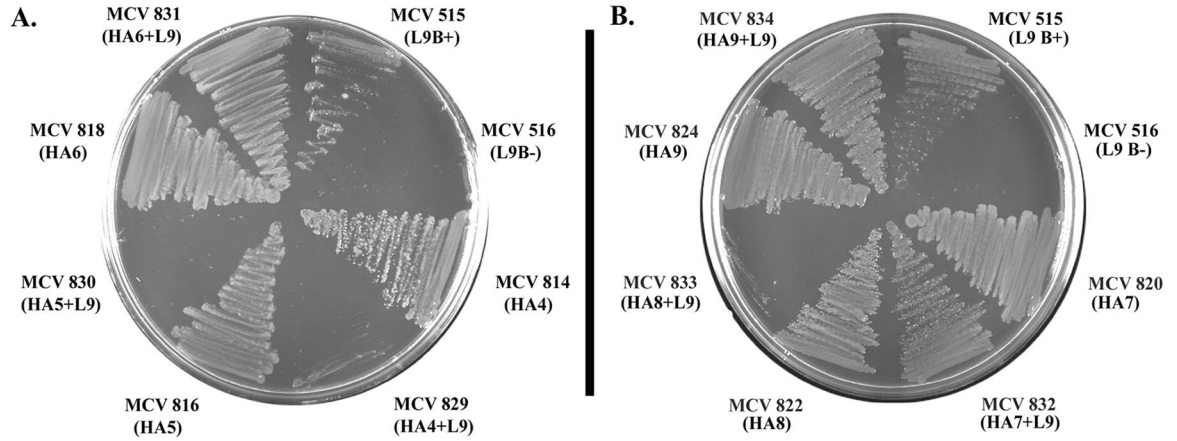

FIG. 8. Growth on Tf as a sole iron source. Gonococcal mutants were plated onto CDM medium containing 30% saturated Tf as a sole iron source. Strains names are listed with the HA epitope insertion number in parentheses. L9 represents the position of the HA insertion in TbpA. MCV515 serves as the positive control strain, and MCV516 serves as the negative control.

quisition (Table 1). This mutant has an HA epitope in putative loop 9 (L9) of TbpA and binds Tf with wild-type affinity (49). We incorporated the L9 mutation into the TbpB-HA fusion mutants and examined their growth phenotypes on CDM-Tf. Following 18 h of growth, the HA1+L9 and HA2+L9 mutants demonstrated growth patterns similar to the parent strain (MCV515) (data not shown). When the HA3+L9 strain was examined, growth was diminished compared to MCV515. However, following 24 h of growth, the HA3+L9 strain reached parental levels of growth (data not shown). These results indicate that the N-terminal regions disrupted by the HA1, HA2, and HA3 insertions were not necessary for TbpB's compensatory function, as growth of these strains and, therefore iron acquisition, were not hindered. On the other hand, when the HA4+L9 and HA5+L9 strains were examined following 24 h of growth, we noted that these mutants did not grow on Tf as a sole iron source (Fig. 8A). These results suggest that the region defined by HA4 and HA5 is necessary for this compensatory TbpB function. Our findings implicate residues 293 to 328, a region defined by insertions 4 and 5, in providing a function which can ordinarily be accomplished by wild-type TbpA. These 35 residues (293 to 328) apparently play an important role in wild-type Tf binding by TbpB as well as in the function of the Tf iron acquisition system as a whole.

Strains containing HA7+L9 and HA9+L9 demonstrated growth patterns similar to the parent strain MCV515 (Fig. 8B). In contrast, the HA8+L9 mutant did not grow as well as the parent strain, demonstrating a growth pattern similar to the HA4+L9 mutant. The region thus defined by insertion 8 is implicated in compensation for the L9 TbpA defect. These data suggest that wild-type TbpB provides a compensatory function for TbpA and that regions targeted by HA4, HA5, and HA8 are required for this role since their functional inactivation results in an inability to grow on Tf. Overall, these results indicate that Tf binding by both lobes of TbpB is necessary to accomplish the iron-scavenging functions contributed by the wild-type protein.

DISCUSSION

The purpose of this study was to identify surface-exposed Tf-binding domains in native gonococcal TbpB. To accomplish this, nine TbpB-HA fusion strains were constructed. Each of the epitope insertions was well tolerated, including those placed within highly conserved domains of TbpB. Western blot analysis indicated that the TbpB-HA fusion proteins were stably expressed by the gonococcus. The presence of the HA epitope resulted in no detectable growth defect in any of the strains. Overall, these results suggest plasticity within TbpB, as both conserved and variable regions could be subjected to mutagenesis without evidence of toxicity.

The presence of multiple species seen in both the anti-TbpB and anti-HA Western blots has been noted previously with recombinant TbpB protein (31). Price et al. demonstrated that a secondary species was actually truncated TbpB, lacking 110 residues from the N terminus. In our analysis, multiple alternate forms were detected, including a similarly sized secondary species. In the anti-HA Western blot, the HA1 fusion strain did not express these alternate TbpB conformations, most likely because these alternate forms lack N-terminal residues of TbpB. As expected, these species were present when Western blots of the HA1 fusion were probed with an anti-TbpB antibody. These other TbpB species did not bind Tf in this analysis, consistent with results from studies with recombinant TbpB truncations (11, 31). The significance of the other TbpB species is unclear. It is possible that they represent progressive truncations of the protein or that they are alternatively modified TbpB proteins. These apparently smaller forms would most likely not be lipid modified, if they lack the signal II peptidase cleavage site; however, other modifications cannot be ruled out.

TbpB is proposed to be fully surface exposed and tethered to the outer membrane by its lipid moiety. This hypothesis, although not previously experimentally tested, is based on surface binding of Tf and some TbpB-specific antibodies (16, 35). In the current study, we report that TbpB is fully surface exposed. All nine TbpB-HA fusion proteins expressed by *N.*

gonorrhoeae exhibited surface-accessible HA epitope tags. The differences in reactivity with the anti-HA monoclonal antibody could be due to secondary sequence constraints, since the regions surrounding the HA epitope could hinder antibody accessibility. It is also possible that these less accessible epitopes are located within domains that are hidden or blocked by other parts of the protein. Insertions 4, 5, and 8 resulted in diminished Tf binding, and these HA epitopes were apparently the least accessible to the antibody. In contrast, the highly reactive insertions surrounding these critical domains (HA2, HA6, HA7, and HA9) were not necessary for Tf binding. Thus, one could speculate that highly conserved regions are required for Tf-binding function and are either less exposed or more constrained in structure such that antibody access is limited. The corollary to this hypothesis is that the diversity domains, shown recently to be limited to narrow regions of gonococcal TbpB (26), are not critical for ligand binding but are more accessible to antibody. As TbpB is a promising vaccine candidate, it is important to define which domains exhibit the greatest sequence diversity and which are readily surface accessible and critical to native function.

Data presented in the current study indicate that both the N- and C-terminal halves of gonococcal TbpB have the capacity to bind Tf, consistent with internal sequence conservation. Our analysis identified five internally homologous regions within N- and C-terminal halves of TbpB, supporting the hypothesis that TbpB is bilobed (27, 36). Similar structures are exhibited by Tf and lactoferrin, both of which contain internal homology within the N- and C-terminal lobes (4). Homologous domains N3 and C3 of TbpB were targeted for HA insertion mutagenesis. Functional analysis suggested that fusion strains containing HA4 and HA8 (located in N3 and C3, respectively) had similar phenotypes with regard to surface binding, iron internalization, and TbpA compensation. Interruption of either binding site reduced Tf binding but completely eliminated all known biological functions of gonococcal TbpB. Insertional mutagenesis of N4 by HA5 similarly resulted in decreased binding and ablation of all known functions of TbpB. These results highlight the critical contributions that each of these conserved regions provides in the wild-type functions of gonococcal TbpB.

A previous study of TbpA structure-function relationships demonstrated that wild-type TbpB provides a compensatory function for TbpA (49). In order to identify the regions of TbpB necessary for this function, we examined a utilization-defective TbpA mutant that requires wild-type TbpB for iron internalization (49). This mutant, unless provided a wild-type TbpB, cannot utilize Tf but exhibits wild-type levels of Tf binding to the surface, indicating that the initial step in Tf utilization is unaffected (49). TbpB could perhaps provide a stripping function, shared by wild-type TbpA, which allows for the release of iron from Tf. By combining the TbpB-HA fusion mutations with the TbpA L9 mutation, we determined that both of the Tf-binding regions of TbpB were required to compensate for the TbpA defect. It seems unlikely that these Tf-binding domains of TbpB represent sites of interaction with TbpA, given the structural constraints of interaction with two large, distinct proteins, although this possibility was not evaluated in the current study. This is the first identification in *N. gonorrhoeae* of specific TbpB domains that provide a function that is also provided by wild-type TbpA. Furthermore, the findings from this study suggest that the regions of TbpB involved in Tf binding have another function, potentially that of removing iron from Tf. It is possible that binding Tf at both sites in TbpB results in efficient iron release from Tf, leading to increased efficiency of iron internalization in its presence.

We previously proposed that TbpB could increase the efficiency of iron internalization by virtue of the fact that this protein preferentially binds holo-Tf (1, 16). Our current findings, however, indicate that the ability to discriminate between apo and ferrated ligands is not sufficient for wild-type levels of iron uptake. HA4, HA5, and HA8 fusion strains demonstrated decreased iron uptake, although they maintained their ability to specifically and preferentially bind the ferrated ligand. Cumulatively, our results suggest that while discrimination is not essential, binding wild-type amounts of Tf to both N- and C-terminal binding domains is necessary for normal TbpB function.

Close homologues of TbpB do not exist in protein sequence databases, and no crystal structure for TbpB is yet available; therefore, creation of a topology model for TbpB has been hindered. In a recent crystal structure study of the *N. meningitidis* putative lipoprotein GNA1870 (9), Cantini et al. presented a speculative homology structure of the C-terminal half of TbpB. Although GNA1870 does not bind Tf, weak sequence homology is exhibited between these potential vaccine candidates, suggesting similar conformations for the two proteins. The hypothetical model presented suggests that TbpB contains eight beta-strands in each lobe of the protein. Computer analysis indicates that TbpB has the potential for multiple (more than eight) beta-strands (unpublished observations). The regions defined in our analysis by HA insertions 4 and 8 are not present in GNA1870 and do not correspond to the proposed beta-strands. In fact, these conserved regions fall within a flexible region between proposed beta-strands 4 and 5 (9). These results are consistent with the conclusion that sequences conserved among the TbpB proteins within domains N3 and C3 are lacking in GNA1870 and that these regions are critical for the Tf-binding and iron internalization functions uniquely associated with TbpB.

The current study supports the hypothesis that TbpB is fully surface exposed. These studies have important vaccine implications as they may allow us to define surface-exposed Tf-binding epitopes, which could be incorporated into a TbpB-based vaccine (32). By examining the function of TbpB variants in the native bacterium, we have precisely defined the conserved domains necessary for ligand interaction, Tf-iron internalization, and TbpA compensation. The current analysis demonstrated that neither lobe of TbpB is solely responsible for Tf binding, ligand discrimination, or ligand species specificity. Previous studies have suggested that the N terminus is responsible for the majority of protein function (33–35, 38). By expressing mutated forms of TbpB in the gonococcus, we were able to demonstrate that the C terminus also provides a necessary contribution to the wild-type function of TbpB. Our results indicate that while the N- and C-terminal halves of TbpB exhibit similar Tf-binding activities, both domains must be present and functional to achieve the wild-type function of this protein.

ACKNOWLEDGMENTS

Funding for this work was provided by Public Health Service grant R01-AI047141 from the National Institute of Allergy and Infectious Diseases, National Institutes of Health.

We also acknowledge the VCU imaging facility, which is supported in part by NIH grant P30CA16059. DNA sequencing was carried out at the DNA facility of the Iowa State University Office of Biotechnology and the Nucleic Acids Research Facilities of Virginia Commonwealth University.

We gratefully acknowledge Christopher Thomas and P. Frederick Sparling for the contribution of anti-TbpB antiserum. We also acknowledge Mary Kate Yost-Daljev and Mark Delboy for assistance in construction of some mutant strains described in this study.

REFERENCES

1. **Anderson, J. E., P. F. Sparling, and C. N. Cornelissen.** 1994. Gonococcal transferrin-binding protein 2 facilitates but is not essential for transferrin utilization. J. Bacteriol. **176:**3162–3170.
2. **Archibald, F. S., and I. W. DeVoe.** 1980. Iron acquisition by *Neisseria meningitidis* in vitro. Infect. Immun. **27:**322–334.
3. **Archibald, F. S., and I. W. DeVoe.** 1979. Removal of iron from human transferrin by *Neisseria meningitidis*. FEMS Microbiol. Lett. **6:**159–162.
4. **Baker, E. N., and P. F. Lindley.** 1992. New perspectives on the structure and function of transferrins. J. Inorg. Biochem. **47:**147–160.
5. **Beucher, M., and P. F. Sparling.** 1995. Cloning, sequencing, and characterization of the gene encoding FrpB, a major iron-regulated, outer membrane protein of *Neisseria gonorrhoeae*. J. Bacteriol. **177:**2041–2049.
6. **Blanton, K. J., G. D. Biswas, J. Tsai, J. Adams, D. W. Dyer, S. M. Davis, G. G. Koch, P. K. Sen, and P. F. Sparling.** 1990. Genetic evidence that *Neisseria gonorrhoeae* produces specific receptors for transferrin and lactoferrin. J. Bacteriol. **172:**5225–5235.
7. **Boulton, I. C., A. R. Gorringe, N. Allison, A. Robinson, B. Gorinsky, C. L. Joannou, and R. W. Evans.** 1998. Transferrin-binding protein B isolated from *Neisseria meningitidis* discriminates between apo and diferric human transferrin. Biochem. J. **334:**269–273.
8. **Briat, J.-F.** 1992. Iron assimilation and storage in prokaryotes. J. Gen. Microbiol. **138:**2475–2483.
9. **Cantini, F., S. Savino, M. Scarselli, V. Masignani, M. Pizza, G. Romagnoli, E. Swennen, D. Veggi, L. Banci, and R. Rappuoli.** 2006. Solution structure of the immunodominant domain of protective antigen GNA1870 of *Neisseria meningitidis*. J. Biol. Chem. **281:**7220–7227.
10. **Cornelissen, C. N., J. E. Anderson, I. C. Boulton, and P. F. Sparling.** 2000. Antigenic and sequence diversity in gonococcal transferrin-binding protein A. Infect. Immun. **68:**4725–4735.
11. **Cornelissen, C. N., J. E. Anderson, and P. F. Sparling.** 1997. Characterization of the diversity and the transferrin-binding domain of gonococcal transferrin-binding protein 2. Infect. Immun. **65:**822–828.
12. **Cornelissen, C. N., J. E. Anderson, and P. F. Sparling.** 1997. Energy-dependent changes in the gonococcal transferrin receptor. Mol. Microbiol. **26:**25–35.
13. **Cornelissen, C. N., G. D. Biswas, and P. F. Sparling.** 1993. Expression of gonococcal transferrin-binding protein 1 causes *Escherichia coli* to bind human transferrin. J. Bacteriol. **175:**2448–2450.
14. **Cornelissen, C. N., G. D. Biswas, J. Tsai, D. K. Paruchuri, S. A. Thompson, and P. F. Sparling.** 1992. Gonococcal transferrin-binding protein 1 is required for transferrin utilization and is homologous to TonB-dependent outer membrane receptors. J. Bacteriol. **174:**5788–5797.
15. **Cornelissen, C. N., M. Kelley, M. M. Hobbs, J. E. Anderson, J. G. Cannon, M. S. Cohen, and P. F. Sparling.** 1998. The transferrin receptor expressed by gonococcal strain FA1090 is required for the experimental infection of human male volunteers. Mol. Microbiol. **27:**611–616.
16. **Cornelissen, C. N., and P. F. Sparling.** 1996. Binding and surface exposure characteristics of the gonococcal transferrin receptor are dependent on both transferrin-binding proteins. J. Bacteriol. **178:**1437–1444.
17. **Gonzalez, G. C., D. L. Caamano, and A. B. Schryvers.** 1990. Identification and characterization of a porcine-specific transferrin receptor in *Actinobacillus pleuropneumoniae*. Mol. Microbiol. **4:**1173–1179.
18. **Herrington, D. A., and P. F. Sparling.** 1985. *Haemophilus influenzae* can use human transferrin as a sole source for required iron. Infect. Immun. **48:**248–251.
19. **Horton, R. M., Z. L. Cai, S. N. Ho, and L. R. Pease.** 1990. Gene splicing by overlap extension: tailor-made genes using the polymerase chain reaction. BioTechniques. **8:**528–535.
20. **Irwin, S. W., N. Averil, C. Y. Cheng, and A. B. Schryvers.** 1993. Preparation and analysis of isogenic mutants in the transferrin receptor protein genes, *tbpA* and *tbpB*, from *Neisseria meningitidis*. Mol. Microbiol. **8:**1125–1133.
21. **Kellogg, D. S., Jr., W. L. Peacock, Jr., W. E. Deacon, L. Brown, and C. I. Pirkle.** 1963. *Neisseria gonorrhoeae*. I. Virulence genetically linked to clonal variation. J. Bacteriol. **85:**1274–1279.
22. **Kenney, C. D., and C. N. Cornelissen.** 2002. Demonstration and characterization of a specific interaction between gonococcal transferrin binding protein A and TonB. J. Bacteriol. **184:**6138–6145.
23. **Laemmli, U. K.** 1970. Cleavage of structural proteins during the assembly of the head of bacteriophage T4. Nature **227:**680–685.
24. **Legrain, M., A. Findeli, D. Villeval, M.-J. Quentin-Millet, and E. Jacobs.** 1996. Molecular characterization of hybrid Tbp2 proteins from *Neisseria meningitidis*. Mol. Microbiol. **19:**159–169.
25. **Legrain, M., V. Mazarin, S. W. Irwin, B. Bouchon, M.-J. Quentin-Millet, E. Jacobs, and A. B. Schryvers.** 1993. Cloning and characterization of *Neisseria meningitidis* genes encoding the transferrin-binding proteins Tbp1 and Tbp2. Gene **130:**73–80.
26. **Martin, I. M., C. A. Ison, D. M. Aanensen, K. A. Fenton, and B. G. Spratt.** 2004. Rapid sequence-based identification of gonococcal transmission clusters in a large metropolitan area. J. Infect. Dis. **189:**1497–1505.
27. **Mazarin, V., B. Rokbi, and M.-J. Quentin-Millet.** 1995. Diversity of the transferrin-binding protein Tbp2 of *Neisseria meningitidis*. Gene **158:**145–146.
28. **Mickelsen, P. A., and P. F. Sparling.** 1981. Ability of *Neisseria gonorrhoeae*, *Neisseria meningitidis*, and commensal *Neisseria* species to obtain iron from transferrin and iron compounds. Infect. Immun. **33:**555–564.
29. **Moeck, G. S., B. S. Bazzaz, M. F. Gras, T. S. Ravi, M. J. Ratcliffe, and J. W. Coulton.** 1994. Genetic insertion and exposure of a reporter epitope in the ferrichrome-iron receptor of *Escherichia coli* K-12. J. Bacteriol. **176:**4250–4259.
30. **Neilands, J. B.** 1981. Microbial iron compounds. Annu. Rev. Biochem. **50:**715–731.
31. **Price, G. A., M. M. Hobbs, and C. N. Cornelissen.** 2004. Immunogenicity of gonococcal transferrin binding proteins during natural infections. Infect. Immun. **72:**277–283.
32. **Price, G. A., M. W. Russell, and C. N. Cornelissen.** 2005. Intranasal administration of recombinant *Neisseria gonorrhoeae* transferrin binding proteins A and B conjugated to the cholera toxin B subunit induces systemic and vaginal antibodies in mice. Infect. Immun. **73:**3945–3953.
33. **Renauld-Mongenie, G., L. Lins, T. Krell, L. Laffly, M. Mignon, M. Dupuy, R.-M. Delrue, F. Guinet-Morlot, R. Brasseur, and L. Lissolo.** 2004. Transferrin-binding protein B of *Neisseria meningitidis*: sequence-based identification of the transferrin-binding site confirmed by site-directed mutagenesis. J. Bacteriol. **186:**850–857.
34. **Renauld-Mongenie, G., M. Latour, D. Poncet, S. Naville, and M. J. Quentin-Millet.** 1998. Both the full-length and the N-terminal domain of the meningococcal transferrin-binding protein B discriminate between human iron-loaded and apo-transferrin FEMS Microbiol. Lett. **169:**171–177.
35. **Renauld-Mongenie, G., D. Poncet, L. von Olleschik-Elbheim, T. Cournez, M. Mignon, M. A. Schmidt, and M.-J. Quentin-Millet.** 1997. Identification of human transferrin-binding sites within meningococcal transferrin-binding protein B. J. Bacteriol. **179:**6400–6407.
36. **Retzer, M. D., R.-H. Yu, and A. B. Schryvers.** 1999. Identification of sequences in human transferrin that bind to the bacterial receptor protein, transferrin-binding protein B. Mol. Microbiol. **32:**111–121.
37. **Retzer, M. D., R.-H. Yu, Y. Zhang, G. C. Gonzalez, and A. B. Schryvers.** 1998. Discrimination between apo and iron-loaded forms of transferrin by transferrin binding protein B and its N-terminal subfragment. Microb. Pathog. **25:**175–180.
38. **Rokbi, B., G. Maitre-Wilmotte, V. Mazarin, L. Fourrichon, L. Lissolo, and M. J. Quentin-Millet.** 1995. Variable sequences in a mosaic-like domain of meningococcal Tbp2 encode immunoreactive epitopes. FEMS Microbiol. Lett. **132:**277–283.
39. **Schryvers, A. B.** 1989. Identification of the transferrin- and lactoferrin-binding proteins in *Haemophilus influenzae*. J. Med. Microbiol. **29:**121–130.
40. **Schryvers, A. B., and G. C. Gonzalez.** 1990. Receptors for transferrin in pathogenic bacteria are specific for the host's protein. Can. J. Microbiol. **36:**145–147.
41. **Schryvers, A. B., and L. J. Morris.** 1988. Identification and characterization of the transferrin receptor from *Neisseria meningitidis*. Mol. Microbiol. **2:**281–288.
42. **Seifert, H. S., R. S. Ajioka, D. Paruchuri, F. Heffron, and M. So.** 1990. Shuttle mutagenesis of *Neisseria gonorrhoeae*: pilin null mutations lower DNA transformation competence. J. Bacteriol. **172:**40–46.
43. **Strutzberg, K., L. von Olleschik, B. Franz, C. Pyne, M. A. Schmidt, and G.-F. Gerlach.** 1995. Mapping of functional regions on the transferrin-binding protein (*TfbA*) of *Actinobacillus pleuropneumoniae*. Infect. Immun. **63:**3846–3850.
44. **Thomas, C. E., W. Zhu, C. N. Van Dam, N. L. Davis, R. E. Johnston, and P. F. Sparling.** 2006. Vaccination of mice with gonococcal TbpB expressed in

vivo from Venezuelan equine encephalitis viral replicon particles. Infect. Immun. **74:**1612–1620.
45. **Vonder Haar, R. A., M. Legrain, H. V. J. Kolbe, and E. Jacobs.** 1994. Characterization of a highly structured domain in Tbp2 from *Neisseria meningitidis* involved in binding to human transferrin. J. Bacteriol. **176:**6207–6213.
46. **Welch, S.** 1992. Transferrin: the iron carrier, p. 1–24. CRC Press, Boca Raton, FL.
47. **West, S. E., and P. F. Sparling.** 1985. Response of *Neisseria gonorrhoeae* to iron limitation: alterations in expression of membrane proteins without apparent siderophore production. Infect. Immun. **47:**388–394.
48. **West, S. E. H., and P. F. Sparling.** 1987. Aerobactin utilization by *Neisseria gonorrhoeae* and cloning of a genomic DNA fragment that complements *Escherichia coli fhuB* mutations. J. Bacteriol. **169:**3414–3421.
49. **Yost-Daljev, M. K., and C. N. Cornelissen.** 2004. Determination of surface-exposed, functional domains of gonococcal transferrin-binding protein A. Infect. Immun. **72:**1775–1785.

Editor: D. L. Burns